Earth and Planetary Science Letters 288 (2009) 194–203

Contents lists available at ScienceDirect

Earth and Planetary Science Letters

journal homepage: www.elsevier.com/locate/epsl

Antarctic crustal thickness from satellite gravity: Implications for the Transantarctic and Gamburtsev Subglacial Mountains

Adrienne E. Block [a,b,*], Robin E. Bell [b], Michael Studinger [b]

[a] Department of Earth and Environmental Sciences, Columbia University, 61 Route 9W, Palisades NY 10964, USA
[b] Lamont-Doherty Earth Observatory, 61 Route 9W Palisades, NY 10964, USA

ARTICLE INFO

Article history:
Received 28 April 2009
Received in revised form 21 August 2009
Accepted 9 September 2009

Editor: R.D. van der Hilst

Keywords:
Antarctica
crustal thickness model
Moho
Gamburtsev Subglacial Mountains
Transantarctic Mountains
GRACE

ABSTRACT

Crustal thickness models are fundamental to understand the tectonic evolution of continents and constrain geodynamic models of their physiographic features. Of particular interest in Antarctica are the crustal thickness variations under the Transantarctic Mountains and Gamburtsev Subglacial Mountains, whose formation mechanisms are still debated. We have used a mean, global gravity field from the Gravity Recovery and Climate Experiment (GRACE) to estimate the depth to the Moho in East and West Antarctica through gravity inversion. We then combined the depth to Moho and known topography to estimate the total crustal thickness. Thick crust is resolved along the full length of the Transantarctic Mountains with a maximum crustal thickness of 46 km predicted near the pole and thinner (~40 km) crust in both northern Victoria Land and under the Pensacola Mountains. Within East Antarctica, the model predicts crust over 40 km thick below the Gamburtsev Subglacial Mountains, which may be the result of a Neoproterozoic suture zone underlying the ice sheet. In addition to addressing long-standing questions about the nature of East Antarctica's major mountain ranges, an improved estimate of crustal thickness variability may improve long-wavelength geodynamic and glaciological models of the continent.

1. Introduction

Efforts to unravel the tectonic history of Antarctica have been hindered by a combination of logistical limitations on the collection of geophysical data and ice cover limiting the availability of rock outcrop. Prominent physiographic features of the Antarctic (Fig. 1), such as the Gamburtsev Subglacial Mountains and the Transantarctic Mountains, still lack fundamental observations that are key to testing models of their origin. The Gamburtsev Subglacial Mountains have extremely limited observations; even the rock types comprising them are unknown. Although relatively well studied in outcrop and through geophysical survey, there is still much debate concerning the formation of the Transantarctic Mountains. In both cases, the underlying crust and upper mantle structure are pivotal to understanding the mechanisms responsible for these features and testing proposed models for their formation. In addition to the inherent challenge of Antarctic data scarcity, recent crustal thickness estimates based on seismic methods are often only representative of small areas immediately below seismic stations. Here we add long-wavelength information to the existing knowledge base.

The long-wavelength accuracy of recent satellite gravity missions has made Moho models attainable in even the toughest terrain (e.g. Shin et al., 2007). Here, we use Parker's (1973) iterative inversion technique to model a continuous, long-wavelength Moho under Antarctica using a gravity field from the Gravity Recovery and Climate Experiment (GRACE). This new continent-wide estimate of crustal thickness enables known and new features on the Moho to be interpreted in a broader context, using insights from their relationship with adjacent provinces.

1.1. Antarctic plate setting

The striking tectonic contrast between East and West Antarctica has long been recognized. Dalziel and Elliot (1982) proposed that East Antarctica is a single large cratonic block while West Antarctica was an assemblage of smaller crustal fragments that moved with respect to East Antarctica and each other. More recently, analysis of shear wave velocities highlighted the subsurface distinction between these two regions: the low velocity mantle of West Antarctica, high velocity mantle of East Antarctica with a transition occurring below the Transantarctic Mountains (Morelli and Danesi, 2004, Ritzwoller et al., 2001).

On the surface, the Transantarctic Mountains form a physical and geological boundary between East and West Antarctica, stretching more than 3500 km and reaching elevations over 4000 m. Unlike most mountain ranges of similar extent or elevation, the Transantarctic Mountains formed without collisional tectonism (ten Brink et al., 1997). Models proposed for their formation include thermal buoyancy

* Corresponding author. 108 Oceanography, 61 Route 9W, Palisades NY 10964, USA. Tel.: +1 845 365 8687; fax: +1 845 365 8179.
E-mail address: adrienne@ldeo.columbia.edu (A.E. Block).

0012-821X/$ – see front matter © 2009 Elsevier B.V. All rights reserved.
doi:10.1016/j.epsl.2009.09.022

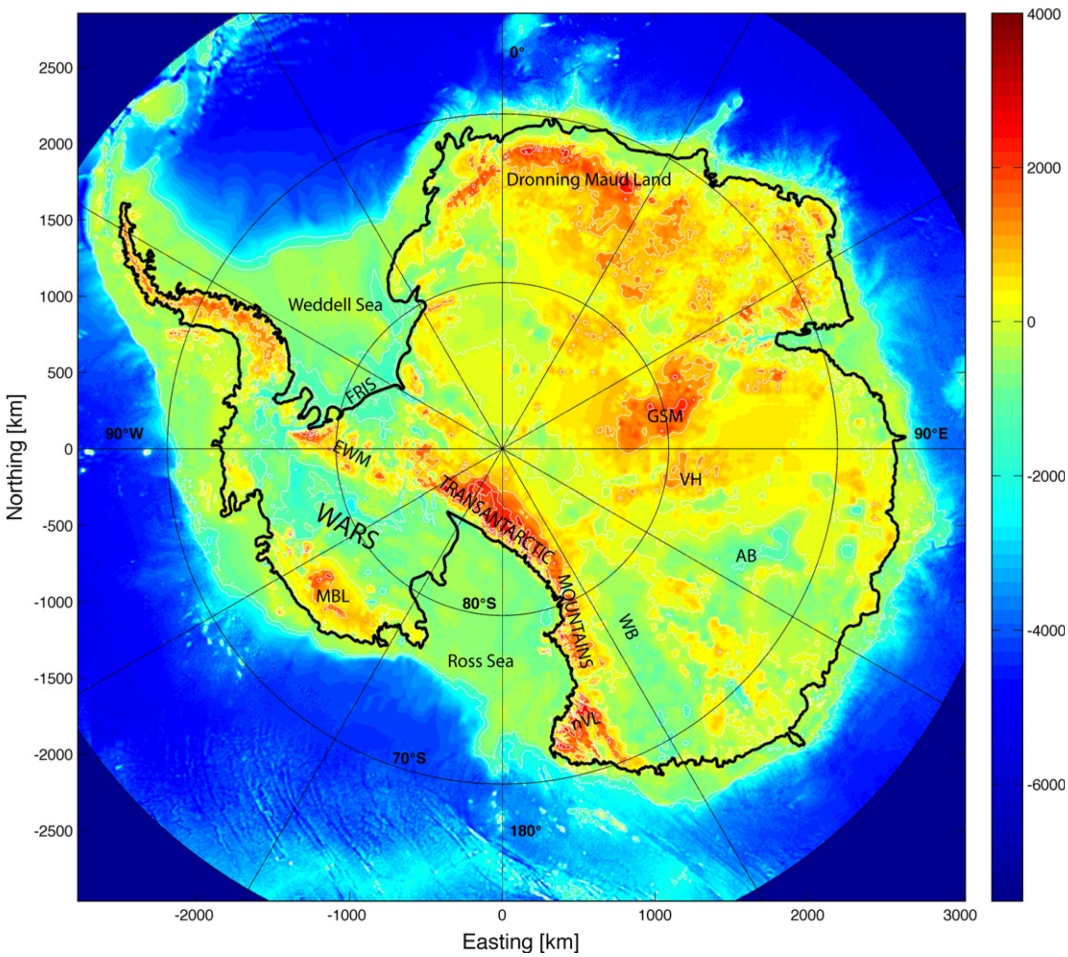

Fig. 1. Bedrock topography grid of Antarctica from BEDMAP (Lythe et al., 2001). Key Antarctic locations are shown: GSM — Gamburtsev Subglacial Mountains. VH — Vostok Highlands. AB — Aurora Basin. WB — Wilkes Basin. nVL — northern Victoria Land. EWM — Ellsworth–Whitmore Mountains. FRIS — Filchner–Ronne Ice Shelf. WARS — West Antarctic Rift System. MBL — Marie Byrd Land.

from an underlying positive temperature anomaly in the upper mantle (ten Brink et al., 1997), thicker crust providing an isostatically buoyant load (Studinger et al., 2004) and, most recently, plateau collapse of a high standing plateau with subsequent uplift and denudation (Bialas et al., 2007). Integrated geophysical analysis has shown that multiple mechanisms must contribute to the elevation of the Transantarctic Mountains; a buoyant load alone cannot explain their height (Studinger et al., 2004; Lawrence et al., 2006).

The prominent tectonic feature of West Antarctica is the West Antarctic Rift System where the main phase of rifting occurred between 105 and 85 Ma but episodic extension has continued into the Cenozoic (Behrendt et al., 1991). Extension within the rift system has left the majority of West Antarctica below sea level, with the exception of Marie Byrd Land and parts of the Antarctic Peninsula. Topographic doming in Marie Byrd Land is attributed to localized hot spot activity (Hole and LeMasurier, 1994; Winberry and Anandakrishnan 2004).

Global and regional scale shear wave velocity models (e.g. Morelli and Danesi, 2004 and references therein; Ritzwoller et al., 2001) resolve little structural variation within East Antarctica due to sparse data coverage and limited resolution. Conversely, coastal rock outcrops have been identified as cratonic fragments with counterparts in India, Africa or Australia. Recent work in the Lambert Glacier region provides evidence for a complex assemblage of diverse terranes and crustal thickness that varies by as much as 9 km across distances of just over 120 km (Reading, 2006). The extent of these cratonic fragments and the trends of the associated orogenic events under the ice sheet remain unknown. (Fitzsimons, 2003, Finn et al., 2006).

Due to their location in the center of East Antarctica, the origin and spatial extent of the Gamburtsev Subglacial Mountains have remained enigmatic since their discovery in 1958. Limited magnetic data from satellite and regional geophysical surveys are inconclusive, showing both positive and negative magnetic anomalies over the range. Bentley (1991) interpreted the magnetic low as indicating a shallow Curie depth, however seismic models have not confirmed an associated positive temperature anomaly. Early estimates of crustal thickness based on a local isostatic assumption predicted an overall thickness of 65 km under the mountain range (Groushinsky and Sazhina, 1982).

More recent efforts to assess the crustal thickness of Antarctica include seismic receiver function analysis (e.g. Reading, 2006; Lawrence et al., 2006; Winberry and Anandakrishnan, 2004, among others), gravity inversion from aerogeophysical surveys (e.g. Studinger et al., 2004, etc.) and inversion of satellite gravity from the CHAllenging Mini-Satellite Payload (CHAMP) mission (Llubes et al., 2003). Receiver functions provide precise point estimations of crustal thickness while the work from CHAMP constrains the long-wavelength crustal signature of more than 666 km. Our new crustal thickness estimate fills the 200–666 km range gap between these types of solutions.

2. GRACE and BEDMAP data

A mean GRACE gravity field and the BEDMAP topography model are fundamental inputs into our gravity inversion.

2.1. Gravity data from GRACE

Grace Gravity Model 3C (GGM03C) is a geopotential model produced by the Center for Space Research (Tapley et al., 2007). The model is a time-averaged gravity field containing raw data spanning January 2003 and December 2006. This static signal represents features of the Earth that can be considered constant during the 5-yr lifespan of the GRACE mission. The GGM03C free-air anomalies (Fig. 2A) to degree 200 are used in our model of Antarctic crustal thickness. West Antarctica is characterized by gravity anomalies averaging ~5 mGal with some isolated highs over Marie Byrd Land and along the Peninsula. East Antarctica is characterized by a series of isolated highs of up to 60 mGal coincident with maximum elevations of the Transantarctic and Gamburtsev Subglacial Mountains and by broad regions of negative anomalies (approx. −60 mGal) associated with the Wilkes and Aurora Basins with generally positive anomalies of 5–10 mGal throughout the rest of the region. The GGM03C free-air field contains artifact striping, paralleling lines of constant longitude that originates from the polar orbit of the GRACE satellites.

2.2. BEDMAP topography grid

In 2001, the BEDMAP consortium compiled all Antarctic ice thickness data available at that time to construct a continental ice thickness model, removed these values from the best available surface DEM (Liu et al., 1999) and produced a gridded model of the subglacial

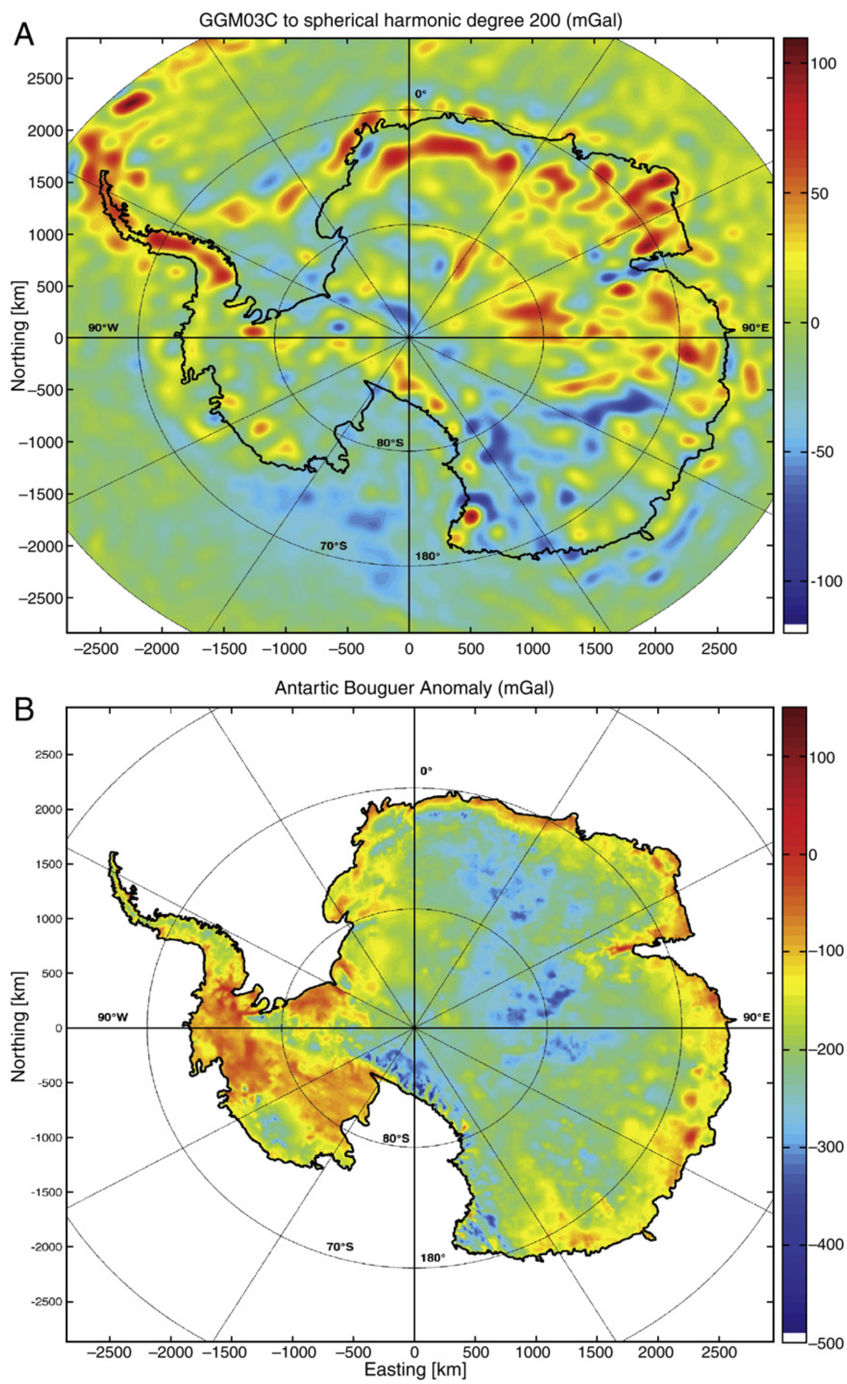

Fig. 2. GRACE gravity fields used to estimate crustal thickness. A.) The GGM03C free-air gravity anomaly. Longitude-parallel striping in the free-air anomaly is an artifact in the GRACE data (Tapley et al., 2005). B.) GRACE-derived Bouguer gravity anomaly.

topography (Fig. 1). Although the compilation included published and unpublished data with over a million kilometers of ground track, the overall data coverage is patchy and inconsistent; some areas have coverage at 10 km spacing, while other areas have coverage at more than 50 km spacing or no data at all. Three major data gaps exist in the BEDMAP data set: one north of the Vostok Highlands along 90°E and the second in Dronning Maud Land between 0° and 30°W, south of 80°S, while a smaller gap centers over Marie Byrd Land. Data scarcity prevented the calculation of a reasonable model for ice thickness over the entire Antarctic; the BEDMAP topography model often relies on a priori assumptions to fill in the data gaps. (Lythe et al., 2001).

3. Inversion method

We begin this section by giving an overview of the Parker–Oldenburg inversion method and the algorithm used in its implementation. In later sections, we detail assumptions made in our inversion, including the assumption of constant density on the ice-rock and Moho interfaces. This later section also discusses the error envelope these assumptions create around our inversion solution.

The forward calculation of gravity anomalies due to topographic variations, h(x,y), on a 2-dimensional surface of uniform density contrast was described in the frequency domain by Parker (1973): $F[\Delta g(x,y)] = -2\pi\gamma\Delta\rho e^{-\bar{k}z_0}\sum_{n=1}^{\infty}\frac{\bar{k}^{n-1}}{n!}F[h^n(x,y)]$ where Δg is the gravity anomaly, γ is the universal gravitational constant, $\Delta\rho$ is the density contrast across the interface, z_0 the mean depth to the surface (positive down) and k the radial wavenumber. Oldenburg (1974) found that the inverse calculation of Parker's (1973) algorithm is: $h(x,y) = F^{-1}\left[\frac{F[\Delta g(x,y)]e^{-\bar{k}z_0}}{-2\pi\gamma\Delta\rho} - \sum_{n=2}^{\infty}\frac{|\bar{k}|^{n-1}}{n!}F[h^n(x,y)]\right]$. The summation term in these algorithms allows relief on the interface to be estimated based on a number of iterations and accounts for a non-linear relationship between gravity and topography.

In 2005, Gomez-Ortiz and Agarwal published 3DINVER.m, a MATLAB code that performs the inverse calculation of Oldenburg (1974) followed by the forward calculation of Parker (1973). The Parker–Oldenburg scheme translates gravity anomalies into topography on an interface and then evaluates the quality of that solution by examining the residual between a Parker forward-modeled gravity field and the one used as input for the Oldenburg algorithm. The script allows up to 10 iterations to be calculated to achieve the desired stability in the topographic solution. We isolated and rearranged the forward and inverse algorithms from the 3DINVER.m code to calculate the Antarctic Bouguer anomaly and invert for topography on the Moho. Iterations were run until successive topography solutions agreed within a fraction of a meter.

To calculate the Bouguer anomaly over Antarctica, we re-gridded the GRACE gravity field into a polar stereographic projection. We then applied Parker's forward algorithm to a layer of ice that effectively removed the gravity contribution of the topography on the air–ice interface. This theoretical layer of ice was added to the existing ice surface producing a level surface at a fixed elevation. Next we must remove the gravity contribution of the density contrast between the ice and the underlying rock; the forward algorithm was employed a second time. We used the density contrast of ice and the underlying rock to fill the space between the bedrock and the level ice surface with rock. At that point, all that remained above sea level was a slab of rock with a constant density. The calculation then proceeded in a traditional way, using a Bouguer slab correction to determine the Bouguer anomaly due to mass variations below the Earth's surface. In contrast to the free-air field (Fig. 2A) that is punctuated by radial GRACE artifacts, the Bouguer anomaly is dominated by major topographic features of Antarctica (Fig. 2B). Finally, the inverse algorithm from 3DINVER.m was implemented to invert the Bouguer anomaly for topography on the Moho.

In order for an inversion solution to converge, one must begin by assuming a mean value for the depth to an interface, z_0, which corresponds to the mean value of the gravity grid. Furthermore, in this application, a low pass filter was applied to prevent numerical instability caused by downward continuing the level of gravity from the surface of the Earth to the mean Moho depth. Since inversion is non-unique, a number of inversion models were calculated. Mean crustal thicknesses outside 32–38 km (see Table 1 entries 4–6) and density contrasts outside the 400–700 kg/m^3 range gave results inconsistent with well known Antarctic features. Only wavelengths shorter than 1000 km were considered part of the crustal signal since the Antarctic geoid, which reflects deeper mantle sources, only provides a significant signal at wavelengths longer than 1000 km. We evaluated models for short wavelength cut-off values from 100 to 225 km, for mean Moho depths between 32 and 38 km and Moho density contrasts of 420–680 kg/m^3. The results of some inversion models are summarized in Table 1. The calculation of various Moho models showed the short wavelength cut-off frequency to be a key parameter, contributing the largest degree of variance to the resulting range of Moho depths. Since we were not able to constrain the wavelength of Moho features using traditional coherence techniques; a range of frequencies consistent with the literature (i.e. Lefort and Agarwal, 2000; Shin et al., 2007) were explored. Although the input GGM03C field has a theoretical resolution of 111 km when expanded to degree and order 360, the GRACE gravity anomaly contains significant power to a 90 km wavelength due to the convergence of longitude near the pole. Allowing shorter wavelengths, between 200 km and 100 km, produces a crustal thickness model with higher frequency content. It is unclear if that higher frequency content represents true variations in crustal thickness or noise introduced by density variations within the crust.

3.1. Model uncertainty

Errors in the depth to Moho model are derived from associated uncertainties in the GRACE gravity field and bedrock topography from BEDMAP as well as the assumptions in the inversion. The total error envelope is at least ± 3 km. This reflects negligible error from GRACE, less than 1 km of error due to BEDMAP inaccuracies and 2 km error due to inversion parameter uncertainty, including the constant densities assumed. Due to selecting inversion parameters consistent

Table 1
Summary results of some inversion model runs in depth to Moho.

Model no.	Mean depth (km)	Band-pass wavelengths (km)	Moho density contrast (kg/m^3)	Minimum depth to Moho (km)	Maximum depth to Moho (km)
1	35	200–1000	500	29.8	44.7
2[a]	35	100–1000	500	28.2	45.0
3[a]	35	150–1000	420	26.9	46.8
4	38	200–1000	500	32.6	47.9
5	32	200–1000	500	26.9	41.4
6	32	200–1000	680	28.3	39.0
7	35	200–1000	420	28.7	46.4
8	35	200–1000	550	30.3	43.8
9	35	200–1000	680	31.2	42.2
10	35	200–3000	500	30.3	44.0
11[b]	35	200–3000	500	30.3	44.0
12[c]	35	666–1000	500	30.9	42.0

Model no. 1 is the model shown and discussed in the figures of this paper. Other model results are included to illustrate sensitivity to inversion parameters. Maximum values occur in the TAM, between the Miller and Horlick ranges. Minimum values occur in the Filchner–Ronne Ice Shelf unless otherwise indicated.

[a] Model uses 150 km or shorter wavelength; requires the use of GRACE to spherical harmonic degree 360.

[b] Model computed with GRACE 360 degree field instead of 200 degree field.

[c] Model run comparable to crustal thickness from CHAMP as published by Llubes et al. (2003).

with known aspects of East Antarctica, we anticipate that the solution in West Antarctica approaches the maximum amplitude of this error. Additional uncertainty due to the distribution of large sedimentary basins could be between .5 km and 4 km.

3.1.1. Data uncertainty

Tapley et al. (2005) calculated the decrease in GGM02C error with increasing spherical harmonic degree. Although the GRACE static gravity field has been updated in the GGM03C model, new estimates of model error are not yet available in the literature. Tapley et al. (2007), state that the GGM03C field is a two-fold improvement over the previous, well-documented GGM02C model. To account for uncertainty, we considered the documented error of the GGM02C field as an upper limit to that of the GGM03C data we have used. Using the GGM02C degree 200 field, the estimated error is less than 10 mm of geoid height or ~4 mGal (Shin et al., 2007). Based on this work, we allow for an uncertainty of no more than 4 mGal for the wavelengths (200–1000 km) of GGM03C used in the inversion.

Being constructed from data with variable spatial resolution, the BEDMAP model uncertainty varies across the continent. The BEDMAP consortium (Lythe et al., 2001) reported elevation errors are typically between 150 and 300 m in continental areas but can be as much as 400 m in mountainous regions. Comparison with subsequent aero-geophysical radar grids showed that while BEDMAP has local inaccuracies of up to 2 km, at longer wavelengths, the error in BEDMAP is generally less than 300 m as reported by Lythe et al. (2001). To evaluate the impact of BEDMAP uncertainty on the GRACE Moho model, values within the topography grid were increased or decreased by 300 m and the Bouguer anomaly and depth to Moho calculation was repeated on the modified grid. Varying the bedrock topography by 300 m contributed less than .63 km of uncertainty in the depth to Moho model.

3.1.2. Inversion parameter uncertainty

The selected density layer model for Antarctica has an ice sheet of 917 kg/m^3 (consistent with the density assumed by Lythe et al. (2001)), overlying a rock layer of density 2700 kg/m^3, and underlain by a mantle of 3300 kg/m^3. In our work, the density contrast on the Moho is modeled as 500 kg/m^3 rather than as the difference of the topographic and mantle layers, to allow for an increase in crustal density under confining pressures. Shear wave velocity studies published by Ritzwoller et al. (2001) and Morelli and Danesi (2004), show that the mantle velocity is different in East and West Antarctica and also changes with depth. The transition is particularly large in amplitude and parallel to the Transantarctic Mountains at 80 km depth and weaker at both shallower and deeper depths. In the uppermost mantle, Ritzwoller et al. (2001) predict variability throughout Antarctica of no more than $\pm 2\%$ with respect to the 1-D velocity model, AK135. Using the basic equations for the velocity of a shear wave, we estimate that density contrast of the Moho is everywhere within ~130 kg/m^3 of the AK135 predicted upper mantle value of 2976 kg/m^3. Since the spatial distribution of the Moho velocity changes is poorly constrained by the current distribution of passive seismic arrays, we have not tried to mimic the spatial variability of the Moho in our model. Instead, we have centered our estimate on a reasonable value for the Moho density contrast and modeled the effect of the predicted variability as uncertainty around our solution. We adopted a reasonable estimate for Moho density contrast of 500 kg/m^3. We suggest that a 130 kg/m^3 envelope around the mean Moho density contrast is consistent with the work of Ritzwoller et al. (2001). This variability contributes an error envelope of ± 1.7 km to all depths reported in the model (see Table 1, entries 7–9).

3.1.3. Sediment distribution

The distribution and thickness of subglacial sediments is unknown throughout most of the Antarctic continent. Estimates of sediment thickness have concentrated around areas of ice streaming in both East and West Antarctica where the presence of sediment modulates ice flow velocities. Among these estimates, Bamber et al. (2006) and Shepherd et al. (2006) have found evidence for 3 km of sediment below East Antarctic Ice Streams, Bell et al. (1998) modeled between 1 km and 2.4 km of sediment below West Antarctic ice streams while Anadakrishnan et al. (1998) estimated only 400–600 m of sediment ~100 km away at the onset of streaming ice. Sediment thickness estimates in the deep interior are rare, however Studinger et al. (2003) have predicted 10 km of sediment in a 400 km area west of Lake Vostok. The gravity anomaly associated with sedimentary basins can be either positive or negative depending on the overall feature size and strength of the lithosphere during rifting and infill (Karner et al., 2005). Since we are using a fixed ice-rock surface topography, the depth to geologic basement cannot be distinguished from the surface of a sedimentary basin. While 400–600 m of sediment contributes less than .5 km uncertainty to Moho depth, 3 km of sediment contributes 1.5 km of uncertainty and the 10 km predicted at Lake Vostok contributes 4 km of uncertainty in Moho depths. Some of the uncertainty due to the presence of sediments will trade-off with the inversion parameter uncertainty described above; total uncertainty is not simply the sum of these two effects. Without a 2-dimensional model of sediment cover, the total uncertainty of the GRACE Moho model is difficult to characterize spatially; regional models that consider known geology could produce better-constrained results.

4. The Moho model

The Moho model (Fig. 3A) is representative of the suite of calculated continental-scale models. This preferred estimate assumes a mean depth to Moho of 35 km and a constant density contrast in both East and West Antarctica. We selected a band-pass of wavelengths between 200 km and 1000 km, assuming that features of this wavelength are on the Moho rather than due to subsurface loads or deeper mantle density anomalies. The use of a 35 km mean crustal thickness limits the reasonable extent of the model to areas within the Antarctic continental shelf. In addition, regions where BEDMAP data coverage is absent (i.e. Marie Byrd Land, north of Vostok Highlands and south of Coats Land) or that contain thick sedimentary sequences (i.e. the Ross and Weddell Seas) are not well represented in the model. Though the model may display a continuous Moho in these regions, we have not interpreted the results in these poorly constrained areas and have covered the solution with a grid.

Total crustal thickness (Fig. 3B) merges the depth to Moho and the surface topography. In addition to uncertainties discussed above, this continent-wide estimate of crustal thickness is subject to the errors of the BEDMAP surface, which can be up to 400 m (Lythe et al., 2001). Thus the total error of the crustal thickness model is larger, ± 3.4 km. Throughout the model description and ensuing discussion, all numeric values are given as total crustal thickness (Fig. 3B).

4.1. Crustal thickness model description

The crust of West Antarctica is thinnest in the region directly below the West Antarctic Rift System (Fig. 3B). The model shows relatively thin (~30 km) crust through central West Antarctica to the base of the Antarctic Peninsula. Crustal thickness in the Peninsula

Fig. 3. Model results. A.) Depth to Moho and B.) total crustal thickness. Total crustal thickness combines depth to Moho and surface topography from the BEDMAP topography grid of Lythe et al. (2001). Hatchured areas lack sufficient BEDMAP constraint and have not been interpreted as part of this work. Numbers indicate other estimates of crustal thickness as described in the text. Locations are abbreviated: WARS — West Antarctic Rift System, EWM — Ellsworth–Whitmore Mountains, SR — Shackleton Range, PM — Pensacola Mountains, HR — Horlick Mountains, MR — Miller Range, WB — Wilkes Basin, GSM — Gamburtsev Subglacial Mountains, VH — Vostok Subglacial Highlands, PB — Prydz Bay.

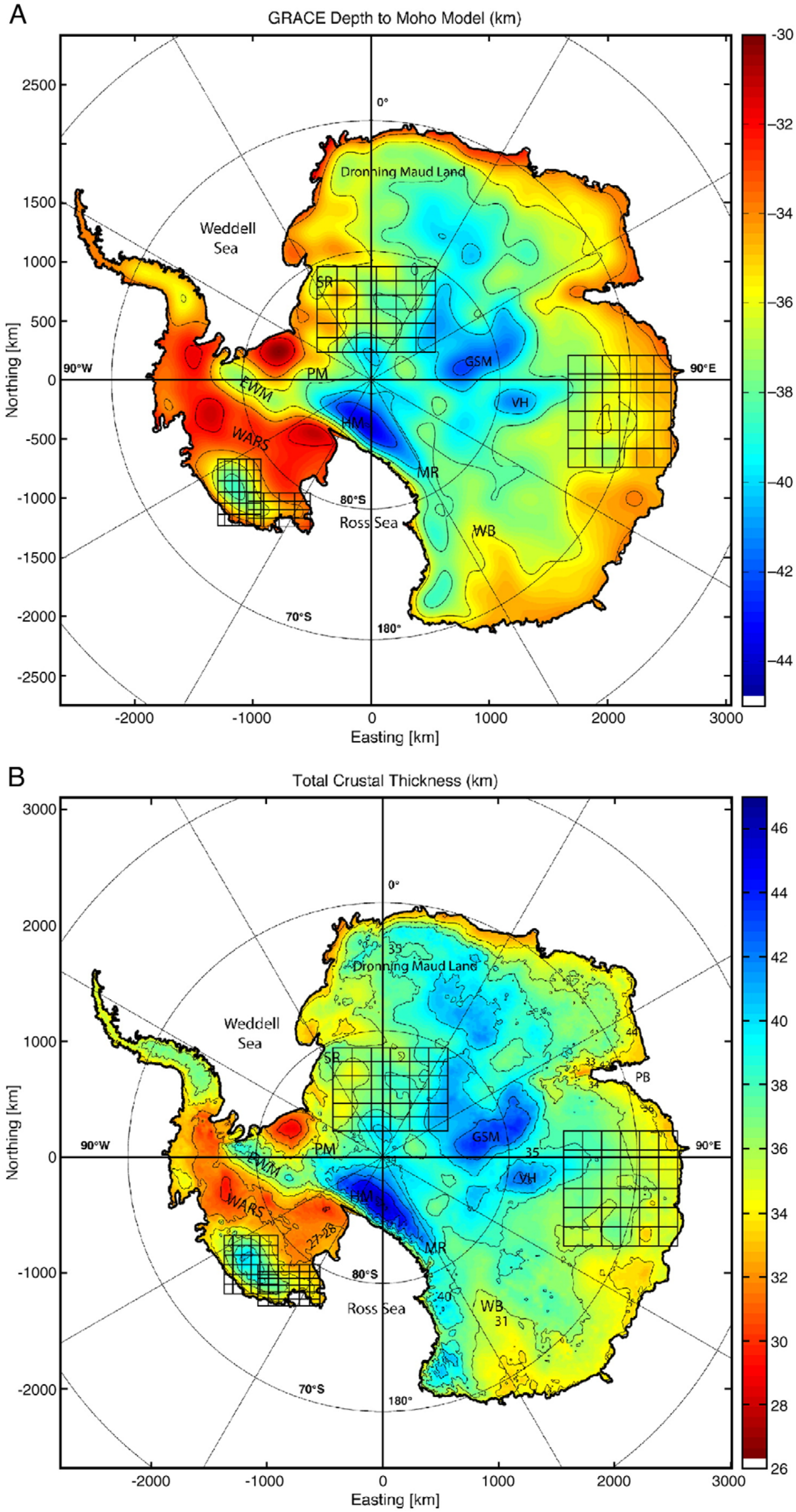
A
GRACE Depth to Moho Model (km)
Dronning Maud Land
Weddell Sea
SR
PM
EWM
WARS
HM
GSM
VH
MR
WB
Ross Sea
0°
90°W
90°E
80°S
70°S
180°
Northing [km]
Easting [km]
B
Total Crustal Thickness (km)
PB
Northing [km]
Easting [km]

reaches a maximum of just less than 37 km but thin to less than 35 km near the northern tip.

Crustal thickness varies along the Transantarctic Mountains. In northern Victoria Land, the crustal thickness is nearly 40 km. Moving South along the Range, some regional thinning of less than 1 km occurs. South of 80°S the range's crust thickens to over 46 km, the maximum crustal thickness predicted in the model. This thick crust underlies the central Transantarctic Mountains between the Horlick and Pensacola Mountains (150°E to ~70°W). Near the pole, the crust also appears to be thicker in the Transantarctic Mountains hinterland. The band of relatively thick crust then jogs northwest toward the Ellsworth-Whitmore Mountains. The crust immediately east and inland of the Filchner–Ronne Ice Shelf is the thinnest crust (29 km) captured by the gravity data.

The crust in East Antarctica is generally thicker than that of West Antarctica. The East Antarctic average crustal thickness of 39 km thins to a coastal average of 34 km. Thicker crust is estimated in Dronning Maud Land at 30°E and extends further south under the Antarctic Plateau and connects to the thick crust that underlies the Gamburtsev Subglacial Mountains, which are represented by a band of 43 km thick crust. South of 80°S, the crust thins to ~37 km between the flanks of the Gamburtsev Subglacial Mountains and the thicker crust of the Transantarctic Mountains hinterland.

4.2. Supporting observations

Prior to GRACE, the CHAMP satellite data were used by Llubes et al. (2003) to estimate a crustal thickness for Antarctica. The CHAMP model shows relatively thin crust in West Antarctica and even thinner crust underlying the Filchner–Ronne Ice Shelf. The crust thickens from the coast of East Antarctica toward the center of the continent. The largest Moho depths are predicted in Dronning Maud Land, under the Gamburtsev Subglacial Mountains and beneath the Transantarctic Mountains near the South Pole. Although the resolution was limited to 666 km, all of the structures of the CHAMP crustal thickness model are also present in the GRACE inversion. (Llubes et al., 2003).

Estimates of crustal thickness in East Antarctica are sparse and many are known to be incorrect due to a lack of constraining seismic data or the use of unrealistic end-member isostasy models. Recent expeditions by the British Antarctic Survey provide some constraints on the coast of Dronning Maud Land between 4°W and 2°E (Ferraccioli et al. (2007) and references therein). Estimates were obtained from the 3D inversion of airborne gravity data. The crust shows a systematic increase in thickness from near shore values of 28 km to inland values of 34–36 km. Similarly, a work in the Lambert Glacier region shows crust thinning from ~40 km to less than 30 km as Prydz Bay is approached (Reading (2006) and references therein). The GRACE Moho model supports this trend, with inland values of ~38 km decreasing towards the coast.

In West Antarctica, the model quality can be compared with seismically defined crustal thickness estimates in the Bentley Subglacial Trench. Winberry and Anandakrishnan (2004) estimate crustal thickness of 27–28 km down the axis of the trench with a general thickening further south near the Transantarctic Mountains. The use of constant values from the Preliminary Reference Earth Model (PREM) for Antarctic P and S wave velocities contributes an estimated uncertainty of 1 km to these estimates.

Additional crustal thickness estimates include an estimate of ~35 km over Lake Vostok (Studinger et al., 2003) and 38 ± 2 km (Bannister et al., 2003) or 40 ± 2 km (Watson et al., 2006) in the Transantarctic Mountains inland from Ross Island. Each of these estimates agrees with our total crustal thickness model.

4.3. Problematic regions

One problematic region in the GRACE Moho model is Marie Byrd Land. Although this region has been well studied in recent years, the topography data coverage in the BEDMAP model was insufficient. We have restricted our interpretation of the tectonic significance of the crustal thickness model to areas in which there are stronger constraints on topography. Winberry and Anandakrishnan (2004) predicted a 25 km thick crust on the southern flank of the Marie Byrd Land topographic high while Luyendyk et al. (2003), predict a gradient in the thickness of the crust, decreasing from 30 km to 25 km thick over a distance of ~100 km. This location illustrates that the 200 km cut-off wavelength assumed in the inversion cannot capture all crustal thickness variation in Antarctica. In the Lambert Graben region of East Antarctica, recent receiver function solutions show changes in crustal thickness of up to 9 km over distances of ~130 km (Reading, 2006). In the GRACE solution, the trend of decreasing crustal thickness is apparent but the relatively dramatic changes revealed by recent seismic work are not. Similarly, the Ross and Weddel seas are problematic both because of an uncharacterized sediment distribution and the existence of known features, such as the Terror Rift, which are too small to detect at the trusted resolution. An alternate model for West Antarctica with a 100 km minimum wavelength for Moho features is shown in Fig. 4. Although the differences are subtle, these shorter wavelength features could be real and represent the region's microplate history.

5. Discussion and implications

5.1. Large-scale patterns in East and West Antarctica

Thinner crust on the margins of East Antarctica reflects the rifting events that separated Antarctica from the other Gondwana landmasses. This thinning is most pronounced on the coast of Dronning Maud Land where Africa and Antarctica diverged.

Due to its thick ice cover, the extent of the West Antarctic Rift System is poorly constrained (Dalziel, 2007). In the crustal thickness model, thinned crust associated with rifting continues north to the base of the Antarctic Peninsula. Considering only wavelengths above 200 km as in Fig. 4A, the crust underlying the rift system appears to thicken only slightly near the coastline. However, when wavelengths as short as 100 km are attributed to the Moho as in Fig. 4B, saddles of thicker crust are more pronounced, particularly along the Bellingshausen Sea margin. The saddles produced at shorter wavelengths may reflect regional variations in rift-related thinning rather than marking the absolute termination of rifting. Without further insights to the wavelength of potential subsurface loads, this model cannot constrain the West Antarctic Rift System's width, but in either scenario, the thinned crust reaches into the narrowed portion of the Antarctic Peninsula.

5.2. The Transantarctic Mountains

Many geologic interpretations indicate that the Transantarctic Mountains extend north toward Coats Land (Fig. 5). In the crustal thickness model, the thick crust of the Transantarctic Mountains does not turn northeast under the Pensacola Mountains, but instead jogs northwest passing under the Whitmore and Ellsworth Mountains. One hypothesis for the origin of the Ellsworth Mountains is that they were once part of the Transantarctic Mountains but were rotated away from the Pensacola Mountains (Storey et al., 1996). The very thin crust underlying the Filchner–Ronne Ice Shelf indicates a region of heightened extension and may be where the rotational separation of the Ellsworth–Whitmore crustal block was accommodated.

The Transantarctic Mountains have crust 4–9 km thicker than their hinterland, with the region of thickest crust correlating with the youngest known basement rocks (1500–1100 Ma; Fitzsimons, 2003). The persistence of thick crust along the range invokes isostatic mechanisms; the topography is not supported by the strength of the lithosphere. The variation in crustal thickness under the range

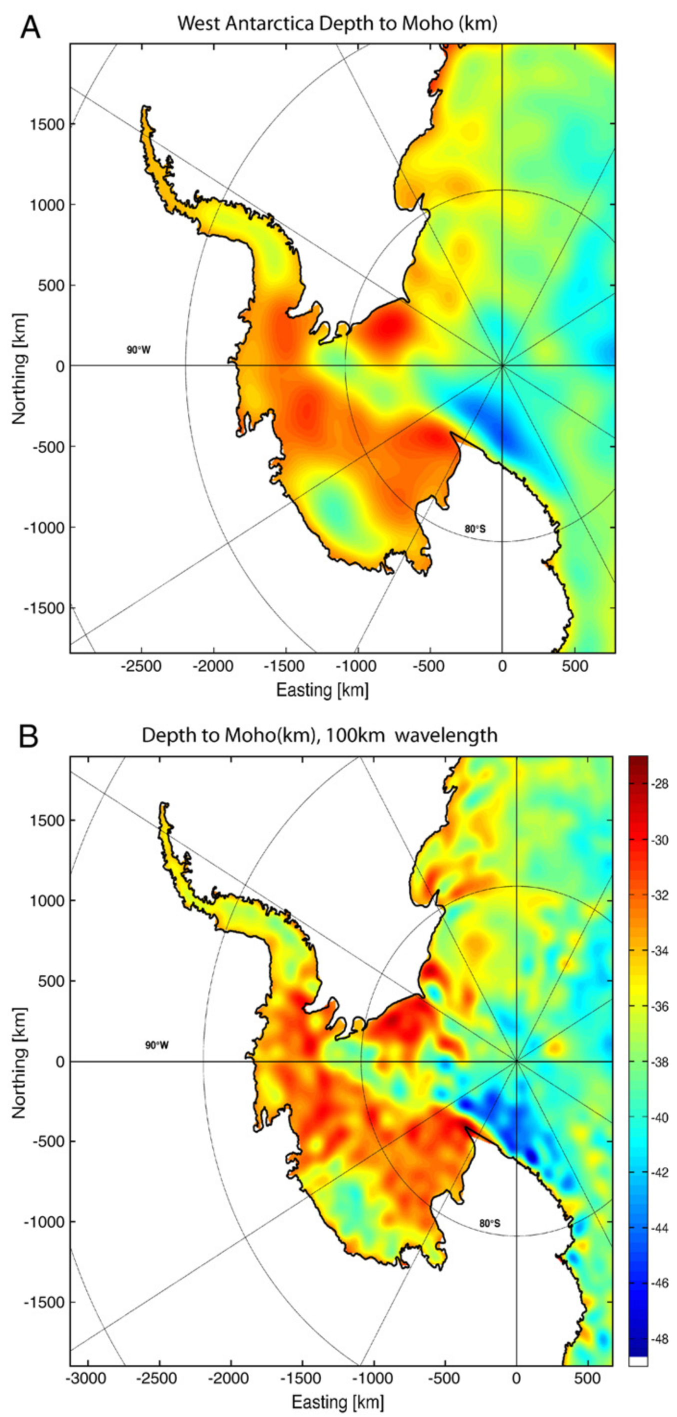

Fig. 4. Comparison of 200 km and 100 km wavelength inversions in West Antarctica. Preferred, 200 km (A) and 100 km (B) versions are plotted at the same color scale.

suggests that the cooperating mechanisms of thermal and isostatic buoyancy vary in importance along strike. The plateau collapse theory advanced by Bialas et al. (2007) suggests that a regional plateau of thickened crust rifted leaving the steep face between the low lying West Antarctic Rift System and the Transantarctic Mountains as a remnant edge of that high standing plateau. The plateau collapse model requires the entire range to sit on thick crust even after allowing for some crustal thinning under the Transantarctic Mountains due to subsequent denudation and uplift. Our new crustal thickness estimate shows thick crust under the Transantarctic Mountain range along the entire Ross Sea front. Ranges from Pensacola Mountains to the Shackleton range are not underlain by thick crust and may have been overprinted by rifting associated with the removal of the Ellsworth–Whitmore crustal block.

It has been proposed that the Wilkes Subglacial Basin formed as a flexural response to the uplift of the adjacent Transantarctic Mountains (ten Brink et al., 1997). Both the presence of thick crust under the length of the TAM and the thinner crust predicted in the Wilkes Subglacial Basin are in conflict with a flexural origin (Studinger et al., 2004, 2006). The flexural model requires a thickened crust of nearly 45 km in the basin and no crustal thickening in the Transantarctic Mountains (ten Brink et al., 1997, Studinger et al., 2004, 2006). Alternatively, the Wilkes Subglacial Basin has been attributed to continental rifting, resulting in a thinned crust below the regionally low topography. The presence of thinner crust than that in the adjacent Transantarctic Mountains is characteristic of the entire basin North of ~82°S, but most pronounced near the coast.

5.3. Gamburtsev Subglacial Mountains

The Pinjarra orogenic event is thought to be responsible for the Neoproterozoic assemblage of East Gondwana, though the only constraints on the orogen path or extent within Antarctica are coastal outcrops (Fitzsimons, 2003). The orogen path must include Prydz Belt, which represents an Ediacaran–Cambrian suture formed by the amalgamation of Indo-Antarctic and Australo-Antarctic continental blocks (Liu et al., 2006). Fitzsimons (2003) proposed three paths of the Pinjarra Orogen under the East Antarctic Ice Sheet, two of which pass through the Gamburtsev Subglacial Mountains and purport a collisional origin for their topography. Kelsey et al. (2008) analyzed detrital zircon from Prydz Belt and concluded that the suture passing through the Gamburtsev Subglacial Mountains and ending in between the Miller and Shackleton sections of the central Transantarctic Mountains was best supported by the geology. Additional support for this orogen path is derived from the similarity of basement age (1100–1000 Ma) in the rocks of Prydz Bay and the Transantarctic Mountains between the Pensacola and Horlick Ranges (Fitzsimons 2003), where our model predicts the thickest Antarctic crust.

Generally, suture zones form parallel to the contact between the plates whose convergence caused their formation and the resulting mountain ranges are underlain by thickened crust. Our crustal thickness model shows bands of thicker crust in East Antarctica, one of which includes the Gamburtsev Subglacial Mountains. The band of thick crust underlying the Gamburtsev Subglacial Mountains is subparallel to one of the proposed paths of the Pinjarra Orogen (Fig. 5), lending support to the idea of the range being a Neoproterozoic suture between disparate parts of East Gondwana. Studinger et al. (2003) modeled the formation of the Lake Vostok Basin as the reactivation of thrust faults that had overridden a passive continental margin. The motion of convergence in those conceptual models is also subparallel to that implied by the elongation of thickened crust and consistent with the same proposed Pinjarra Orogen path.

Alternative models for the Gamburtsev Subglacial Mountains suggest they are the result of thermal uplift, similar to the Precambrian Hoggar Massif of northwest Africa, or are an erosional remnant resulting from differential erosion under a basaltic capping. If the Gamburtsev Subglacial Mountains are supported by magmatic underplating then the largest mass deficit, represented in the model as the thickest crust, should underlie the region of highest topography. In our model, the largest mass deficit is not coincident with the Gamburtsev Subglacial Mountains' highest known peaks but is offset toward the interior, consistent with other global examples of collisional mountain ranges (Karner and Watts, 1983). Without better bedrock constraints, it is difficult to know how high the Gamburtsev Subglacial Mountains stand above the local background topographic level but, in the present data, they do not have the domal structure and rough radial symmetry associated with both continental and oceanic

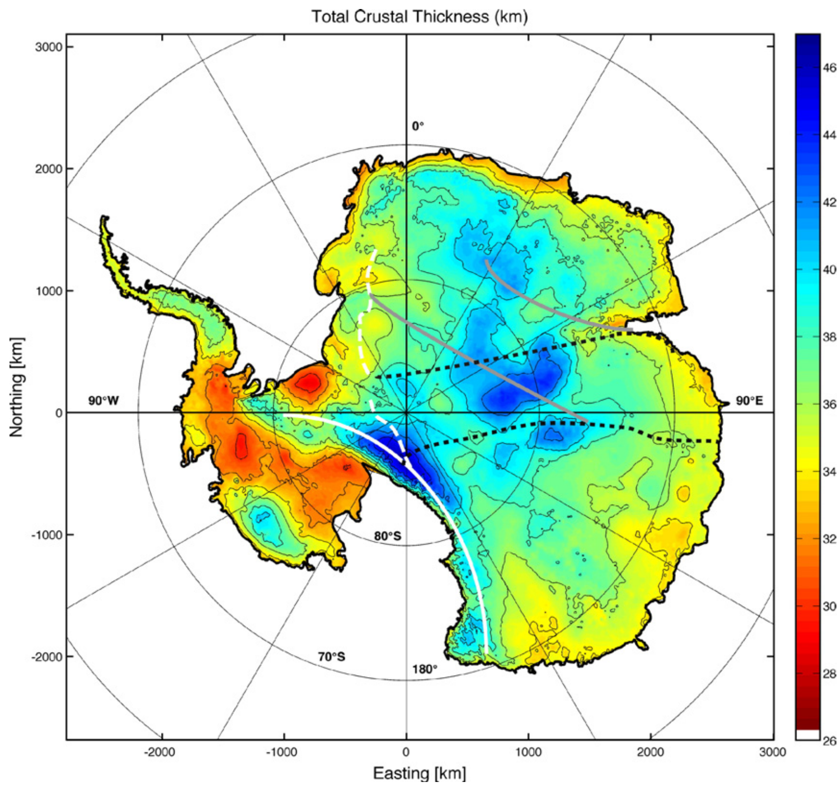

Fig. 5. Large-scale tectonic trends. Path of the Transantarctic Mountains (dashed white line) and West Antarctic Rift System shoulder (solid white line) after Behrendt and Cooper (1991). Also shown are 2 proposed paths of the Pinjarra Orogen after Fitzsimons (2003). The black stippled orogen path is best supported by these data.

hot spot domes (Crough, 1981). Although these mountains have not been dated through direct sampling, van de Flierdt et al. (2007) have tentatively assigned an age of 500 Ma to the range, based on the assumption that Prydz Bay sediments are derived from the slopes of these mountains. This work places the mountains' formation in a stage of final Gondwana assembly and may exclude the possibility that the mountains are formed by recent hotspot activity. Furthermore, the thermal doming hypothesis requires the persistence of a buoyant load, which can be tested by analysis of seismic data being collected at this time (GAMSEIS project, Wiens et al., ongoing). Prior volcanism, resulting in the formation of an erosion-resistant neck cannot be ruled out by these observations.

To date, the elevated relief of the Gamburtsev Subglacial Mountains has been the primary constraint on their history as well as their most enigmatic observation. The results of our crustal thickness estimate indicate a band of thickened crust aligned under the elevated topography of the range. While 42–43 km thick crust beneath the Gamburtsev Subglacial Mountains is distinct from the average 37 km thick crust of the East Antarctic interior, this crust is significantly thinner than the almost 50 km thick crust predicted in other gravity-based studies (e.g. von Frese et al., 1999). Globally, modern mountain ranges like the Alps have high relief and are underlain by over-thickened crust while older ranges like the Appalachians have a subdued surface expression and lack crustal roots (Nelson, 1992 and references therein). The Gamburtsev Subglacial Mountains do not comply with either end member; they present a raised topography in the absence of a significant crustal root. In the Eastern Pyrenees, the mountain peaks are anomalously high with respect to their subdued crustal roots. This has been attributed to Neogene reactivation of the range in response to lithospheric thinning. (Gunnel et al., 2008). While the Gamburtsev Subglacial Mountains crustal root may have formed during convergent tectonics associated with the assembly of Gondwana and recorded in the outcrop geology in the Prydz Bay region (Fitzsimons, 2003), an additional tectonic event, possibly reactivation of this older structure, is necessary to explain their modern relief.

6. Conclusions

Time-averaged GRACE satellite data was used to calculate a new continent-wide estimate of crustal thicknesses in Antarctica. In turn, this model can be used to constrain seismic and geodynamic investigations that previously employed unrealistic a priori models of crustal thickness.

The crustal thickness model shows that thinned crust associated with West Antarctic Rift System extends to the Antarctic Peninsula. Along the Transantarctic Mountains the maximum crustal thickness is located proximal to the South Pole, in the region of youngest basement age. The degree of correlation of Moho depth with topographic height along the range reinforces previous work suggesting that isostasy is not the only mechanism supporting the range. No single mechanism is responsible for the uplift and support of the Transantarctic Mountains. The plateau collapse model for the Transantarctic Mountains' formation requires a thicker crust under the entire range as predicted by our crustal thickness model. A prominent zone of thickened crust also underlies the Gamburtsev Subglacial Mountains. This crustal root may be the result of East–West oriented suturing that formed East Gondwana.

The debate over the Gamburtsev Subglacial Mountains' origins has persisted for decades due to a lack of data on which to base arguments for the models. Most theories are speculative at best. Our results support a collisional origin for the range but their vertical scale requires a later tectonic event to reactivate uplift within the Gamburtsev Subglacial Mountains. Despite a wealth of new information from GRACE, this origin story still requires further testing and analysis as new data is collected. Detailed study in ongoing International Polar Year projects will reveal the composition and full extent of the Gamburtsev Subglacial Mountains. The work undertaken here provides a framework for interpreting those results in the larger context of East Antarctic tectonism.

Acknowledgements

Isabella Velicogna is thanked for discussions and help with GRACE data. Garry Karner contributed to this project in the early phase. Funding for this work was provided by the US National Science Foundation's Office of Polar Programs (Award #0338278 to LDEO). A. Block was supported by an NSF Graduate Fellowship for much of this work. LDEO contribution number 7304.

References

Anadakrishnan, S., Blankenship, D.D., Alley, R.B., Stoffe, P.L., 1998. Influence of subglacial geology on the position of a West Antarctic ice stream from seismic observations. Nature 394, 62–65.

Bamber, J.L., Ferraccioli, F., Joughin, I., Shepherd, T., Rippin, D.M., Sigert, M.J., Vaughan, D.G., 2006. East Antarctic ice stream tributary underlain by major sedimentary basin. Geology 34 (1), 33–36.

Bannister, S., Yu, J., Leitner, B., Kennett, B.L.N., 2003. Variations in crustal structure across the transition from West to East Antarctica Southern Victoria Land. Geophys. J. Int. 155, 870–884.

Behrendt, J.C., Cooper, A.K., 1991. Evidence of rapid Cenozoic uplift of the shoulder escarpment of the Cenozoic West Antarctic rift system and a speculation on possible Climate forcing. Geology 19, 315–319.

Behrendt, J.C., LeMasurier, W.E., Cooper, A.K., Tessensohn, F., Trehu, A., Damaske, D., 1991. Geophysical studies of the West Antarctic Rift System. Tectonics 10, 1257–1273.

Bell, R.E., Blankenship, D.D., Finn, C.A., Morse, D.L., Scambos, T.A., Brozena, J.M., Hodge, S.M., 1998. Influence of subglacial geology on the onset of a West Antarctic ice stream from aerogeophysical observations. Nature 394, 58–62.

Bentley, C.R., 1991. Configuration and structure of the subglacial crust. In: Tingey, R.J. (Ed.), The Geology of Antarctica, vol. 17. Oxford University Press, Oxford, United Kingdom, pp. 335–364.

Bialas, R.W., Buck, W.R., Studinger, M., Fitzgerald, P., 2007. Plateau collapse model for the Transantarctic Mountains West Antarctic Rift System: Insights from numerical experiments. Geology 35 (8), 687–690.

Crough, S.T., 1981. Free-Air gravity over the Hoggar Massif, Northwest Africa: Evidence for alteration of the lithosphere. Tectonophysics 77, 189–202.

Dalziel, I.W.D., Elliot, D.H., 1982. West Antarctica; problem child of Gondwanaland. Tectonics 1 (1), 3–19.

Dalziel, I.W.D., 2007. The Ellsworth Mountains: critical and enduringly enigmatic. In: Cooper, A.K., Raymond, C.R., et al. (Eds.), Antarctica: A Keystone in a Changing World – Online Proceedings of the 10th ISAES, USGS Open-File Report 2007-1047, Short Research Paper 004, 5 p.; doi:10.3133/of2007-1047.srp004.

Finn, C.A., Goodge, J.W., Damaske, D., Fanning, C.M., 2006. Scouting craton's edge in paleo-Pacific Gondwana. In: Fuetterer, D.K., Damaske, D., Kleinschmidt, G., Miller, H., Tessenshon, F. (Eds.), Antarctica; Contributions to Global Earth Sciences; Proceedings: International Symposium on Antarctic Earth Science, vol. 9, pp. 165–173.

Fitzsimons, I.C.W., 2003. Proterozoic basement provinces of southern and southwestern Australia, and their correlation with Antarctica. In: Yoshida, M., Windley, B.E., Dasgupta, S. (Eds.), Proterozoic East Gondwana: Supercontinent Assembly and Breakup: Geol. Soc. London, Special Publications, vol. 206, pp. 93–130.

GAMSEIS project. (Wiens, D. et al.) A broadband seismic experiment to image the lithosphere beneath the Gamburtsev Mountains, East Antarctica (GAMSEIS). http://classic.ipy.org/development/eoi/details.php?id=412.

Gomez-Ortiz, S., Agarwal, B.H.P., 2005. 3DINVER.M: a MATLAB program to invert the gravity anomaly over a 3D horizontal density interface by Parker–Oldenburg's algorithm. Comput. Geosci. 31, 513–520.

Groushinsky, N.P., Sazhina, N.B., 1982. Some features of Antarctic crustal structure. In: Craddock, C.C. (Ed.), Antarctic Geoscience. University of Wisconsin Pres, Madison. 1172 pp.

Gunnel, Y., Zeyen, H., Calvet, M., 2008. Geophysical evidence of a missing lithospheric root beneath the Eastern Pyrenees: Consequences for post-orogenic uplift and associated geomorphic signatures. Earth Planet. Sci. Lett. 276, 302–313.

Hole, M.J., LeMasurier, W.E., 1994. Tectonic controls on the geochemical composition of Cenozoic, mafic alkaline volcanic rocks from West Antarctica. Contrib. Mineral. Petrol. 117 (2), 187–202.

Karner, G.D., Watts, A.B., 1983. Gravity anomalies and flexure of the lithosphere at mountain ranges. J. Geophys. Res. 88 (B12), 10,449–10,477.

Karner, G.D., Studinger, M., Bell, R.E., 2005. Gravity anomalies of sedimentary basins and their mechanical implications: application to the Ross Sea basins, West Antarctica. Earth Planet. Sci. Lett. 235, 577–596.

Kelsey, D.E., Wade, B.P., Collins, A.S., Hand, M., Sealing, C.R., Netting, A., 2008. Discovery of a Neoproterozoic basin in the Prydz belt in East Antarctica and its implications for Gondwana assembly and ultrahigh temperature metamorphism. Precambrian Res. 161, 355–388.

Lawrence, J.F., Wiens, D.A., Nyblade, A., Anandakrishnan, S., Shore, P.J., Voigt, D., 2006. Crust and upper mantle structure of the Transantarctic Mountains and surrounding regions from receiver functions, surface waves, and gravity: implications for uplift models. Geochem. Geophys. Geosyst. 7.

Lefort, J.P., Agarwal, B.N.P., 2000. Gravity and geomorphological evidence for a large crustal bulge cutting across Brittany (France): a tectonic response to the closure of the Bay of Biscay. Tectonophysics 323, 149–162.

Liu, H.X., Jezek, K.C., Li, B., 1999. Development of an Antarctic digital elevation model by integrating cartographic and remotely sensed data: a geographic information system based approach. J. Geophys. Res. 104 (B10), 23,199–23,213.

Liu, X., Jahn, B., Zhao, Y., Li, M., Li, H., Liu, X., 2006. Late Pan-African granitoids from the Grove Mountains, East Antarctica: age, origin and tectonics implications. Precambrian Res. 145, 131–154.

Llubes, M., Florsch, N., Legresy, B., Lemoine, J.M., Loyer, S., Crossley, D., Remy, F., 2003. Crustal thickness in Antarctica from CHAMP gravimetry. Earth Planet. Sci. Lett. 212, 103–117.

Luyendyk, B.P., Wilson, D.S., Siddoway, C.S., 2003. Eastern margin of the Ross Sea Rift in western Marie Byrd Land, Antarctica: crustal structure and tectonic development. Geochem. Geophys.Geosyst. 10 (4).

Lythe, M.B., Vaughan, D.G., BEDMAP consortium, 2001. BEDMAP; a new ice thickness and subglacial topographic model of Antarctica. J. Geophys. Res., B, Solid Earth Planets 106 (6), 11,335–11,351.

Morelli, A., Danesi, S., 2004. Seismological imaging of the Antarctic continental lithosphere: a review. Glob. Planet. Change 42, 155–165.

Nelson, K.D., 1992. Are crustal thickness variations in old mountain belts like the Appalachians a consequence of lithospheric delamination? Geology 20, 498–502.

Oldenburg, D.W., 1974. The inversion and interpretation of gravity anomalies. Geophysics 39 (4), 526–536.

Parker, R.L., 1973. Rapid calculation of potential anomalies. Geophys. J. R. Astron. Soc. 31 (4), 447–455.

Reading, A.M., 2006. The seismic structure of Precambrian and early Paleozoic terranes in the Lambert Glacier region East Antarctica. Earth Planet. Sci. Lett. 244, 44–57.

Ritzwoller, M.H., Shapiro, N.M., Levshin, A.L., Leahy, G.M., 2001. Crustal and upper mantle structure beneath Antarctica and surrounding oceans. J. Geophys. Res., B, Solid Earth Planets 106 (12), 30,645–30,670.

Shepherd, T., Bamber, J.L., Ferraccioli, F., 2006. Subglacial geology in Coats Land, East Antarctica, revealed by airborne magnetics and radar sounding. Earth Planet. Sci. Lett. 244, 323–335.

Shin, Y.H., Xu, H., Braitenburg, C., Fang, J., Wang, Y., 2007. Moho undulations beneath Tibet from GRACE-integrated gravity data. Geophys. J. Int. 170, 971–985.

Storey, B.C., Vaughan, A.P.M., Millar, I.L., 1996. Geodynamic evolution of the Antarctic Peninsula during Mesozoic times and its bearing on Weddel Sea history, in: Storey, B.C., King, E.C., and Livermore R.A., (Eds), Weddel Sea Tectonics and Gondwana Break-Up. Spec. Publ.-Geol. Soc vol. 108, 87–103.

Studinger, M., Bell, R.E., Buck, W.R., Karner, G.D., Blankenship, D., 2004. Sub-ice geology inland of the Transantarctic Mountains in light of new aerogeophysical data. Earth Planet. Sci. Lett. 220 (3–4), 391–408.

Studinger, M., Karner, G.D., Bell, R.E., Levin, V., Raymond, C.A., Tikku, A.A., 2003. Geophysical models for the tectonic framework of the Lake Vostok region East Antarctica. Earth Planet. Sci. Lett. 216 (4), 663–677.

Studinger, M., Bell, R.E., Fitzgerald, P., Buck, W.R., 2006. Crustal architecture of the Transantarctic Mountains between the Scott and Reedy Glacier region and South Pole from aerogeophysical data. Earth Planet. Sci. Lett. 250 (1–2), 182–199.

Tapley, B., Ries, J., Bettapur, S., Chambers, D., Cheng, M., Condi, F., Gunter, B., Kang, Z., Nagel, P., Pastor, R., Pekker, T., Pooles, S., Wang, F., 2005. GGM02 — an improved earth gravity field model from GRACE. J. Geod. 79 (8).

Tapley, B., Ries, J., Bettadpur, S., Chambers, D., Cheng, M., Condi, F., Poole, S., 2007. The GGM03 mean earth gravity model from GRACE. Eos Trans. AGU 88 (52) Fall Meet. Suppl., Abstract G42A-03, 2007.

ten Brink, U.S., Hackney, R.I., Bannister, S., Stern, T., Makovsky, Y., 1997. Uplift of the Transantarctic Mountains and the bedrock beneath the East Antarctic ice sheet. J. Geophys. Res.-Solid Earth 102 (B12), 27,603–27,621.

van de Flierdt, T., Gehrels, G.E., Goldstein, S.L., Hemming, S.R., 2007. Pan African age of the Gamburtsev Mountains? In: Cooper, A.K., Raymond, C.R. (Eds.), Antarctica: A Keystone in a Changing World — Online Proceedings of the 10th ISAESX: USGS Open File Report 2007-1047, Extended Abstract, vol. 176. 4 pp.

von Frese, R., Tan, L., Woo Kim, J., Bentley, C., 1999. Antarctic crustal modeling from the spectral correlation of free-air gravity anomalies with the terrain. J. Geophys. Res. 104 (B11), 25275–25296.

Watson, T., Nyblade, A., Wiens, D.A., Anandakrishnan, S., Benoit, M., Shore, P.J., Voigt, D., VanDecar, J., 2006. P and S velocity structure of the upper mantle beneath the Transantarctic Mountains, East Antarctic Craton, and Ross Sea from travel time tomography. Geochem. Geophys. Geosyst. 7.

Winberry, J.P., Anandakrishnan, S., 2004. Crustal structure of the West Antarctic Rift System and Marie Byrd Land Hotspot. Geology 32 (11), 977–980.